Sphingomyelin Structure Influences the Lateral Diffusion and Raft Formation in Lipid Bilayers

Andrey Filippov, Greger Orädd, and Göran Lindblom
Department of Biophysical Chemistry, Umeå University, Umeå, Sweden

ABSTRACT Liquid-disordered/liquid-ordered two-phase coexistence regions in hydrated bilayers have been investigated for sphingomyelins (SMs) of three different origins: egg, brain, and milk with the pulsed-field gradient NMR technique for lateral diffusion measurement. It is found that the three SMs have the same diffusional behavior in bilayers of SM alone, but in the multicomponent systems of dioleoylphosphatidylcholine/SM/cholesterol, the ability to form domains differs for the three SMs. The two-phase area is more extended for egg SM than for brain SM, and no two-phase coexistence is found for milk SM. The differences in behavior are correlated with the homogeneity of the SM hydrocarbon chain compositions, in which egg SM has the most homogeneous and milk SM has the most heterogeneous composition. The results indicate that a crucial element in the domain-forming process is the formation of highly packed bilayers of SM and cholesterol rather than specific interactions between SM and cholesterol.

INTRODUCTION

It is generally accepted that macro- and microdomains exist within the plane and across the two lipid layers of the biological membrane, and that their presence may be associated with important cell functions, such as signal transduction, lipid trafficking, transcytosis, protein sorting, and virus budding (1–3). In the simplest form, such domains occur in systems of two-phase coexistence of the liquid-ordered (l_o) phase, in which the lipids are more tightly packed, and the surrounding liquid-disordered (l_d) phase (4,5). However, the formation of biologically functional domains, also referred to as rafts, requires additional components of lipids or proteins (1). The most common way in which rafts are operationally identified in cellular systems is by extraction with cold detergent (6) with a characteristic enrichment in sphingolipids (SLs) and cholesterol (CHOL) in the insoluble fraction. All types of SL molecules (sphingomyelins, ceramides, gangliosides, neutral glycosphingolipids, and sulfatides) have been detected in detergent resistant fractions and, considering the large variation in chain compositions, an enormous diversification in membrane composition is provided. Although model raft systems without SLs have been observed, bilayers containing SLs seem to produce the most thermodynamically stable lipid domains (7–9).

Sphingolipids appear to have a rather large propensity for self-aggregation and evidence of liquid domain formation also in the absence of CHOL has been found (10). The reason for this can be found in the chemical structure of the SL family. Natural SLs have a long-chain base (LCB) together with an amide-linked acyl chain. The acyl chains in natural sphingomyelins (SMs) are usually highly saturated and vary in length from 16 to 24 carbons, while the LCB has a *trans* double bond between carbons 4 and 5 and the majority species contain 18 carbons. The predominance of saturated acyl chains in the hydrocarbon region contributes to the high phase transition temperature characteristic of SLs.

A major difference between SM and the other major class of lipids, phosphatidylcholine (PC), occurs in the bilayer interfacial region. The PC contains two carbonyls that can act as hydrogen-bond acceptors, while SM exhibits a *trans* double bond, a hydroxyl group, and an amide group in this region. The possibility of the formation of hydrogen bonds has been suggested to be one of the special properties of SLs (11–14) and probably contributes to the small molecular area of SM, compared to that of PC (15–18). This proposal is also supported by recent molecular dynamics simulations (19–21) in which both inter- and intramolecular hydrogen bonding are present, and clustering of up to nine intermolecularly linked SMs are observed.

The interaction between SM and CHOL involves van der Waals stabilization contributed by the planar steroid ring interacting with the hydrocarbon chains of SM, and computer simulations also indicates hydrogen bonding between the 3-OH group of CHOL and the SM (22). Several modifications of the SM molecule have revealed that interactions in the headgroup (23), the interface (24), and the hydrocarbon region (25–27) as well as the stereoconfiguration (28) contribute to the stabilization of domains. To further expand our understanding of the domain-formation process, we have undertaken a study including three different SMs from natural sources, coming from egg, brain, and milk. The three SMs differ only in the hydrocarbon chain compositions and we thus focus our efforts on a study of the importance of the

Submitted September 27, 2005, and accepted for publication December 12, 2005.

Address reprint requests to G. Orädd, Tel.: 46-90-786-53-67; E-mail: greger.oradd@chem.umu.se.

Andrey Filippov's permanent address is Dept. of Molecular Physics, Kazan State University, 420008 Kazan, Russia.

0006-3495/06/03/2086/07 $2.00

doi: 10.1529/biophysj.105.075150

structure of the hydrophobic part of the SM molecule for raft-formation.

The pulsed-field gradient (pfg) NMR method has been used to measure the lipid lateral diffusion in macroscopically oriented bilayers. This method has proven to be very efficient in detecting the formation and dynamics of lipid domains in bilayers (9,29–31).

MATERIALS AND METHODS

Three different SMs of natural origin were used: brain porcine sphingomyelin (bSM, Avanti Polar Lipids, Alabaster, AL); milk bovine sphingomyelin (mSM, Avanti); and chicken egg yolk sphingomyelin (eSM, Sigma, St. Louis, MO and Avanti). The lipid chain compositions in Fig. 1 refer to the Avanti lots. No data are available for the chain composition for the Sigma eSM but it is assumed that it is similar to that of the Avanti eSM. Results obtained from the two eSMs were indistinguishable. The two other lipid components in the mixed bilayers were 1,2-dioleoyl-*sn*-glycero-3-phosphocholine (DOPC, Avanti) and cholesterol, Sigma Grade: 99+% (CHOL, Sigma). Deuterated water (^2H_2O, 99.7%) was purchased from Larodan AB (Malmö, Sweden).

Pulsed-field gradient NMR

Macroscopically aligned lipid bilayers were prepared with equimolar amounts of DOPC and SM, and with CHOL concentrations ranging from 8 to 40 mol %, according to methods described elsewhere (31). To assure excess water conditions, a pool of water was added to filter papers at the ends of the hydrated samples before sealing them.

The ^{1}H NMR diffusion measurements were performed on a Chemagnetics Infinity (Varian, Fort Collins, CO) spectrometer operating at a proton frequency of 100 MHz equipped with a purpose-built goniometer probe that enables samples of macroscopically aligned bilayers to be oriented with the bilayer normal at the magic angle with respect to the main magnetic field. Details of the pfg-NMR method for lipid lateral diffusion measurements and data analysis can be found elsewhere (29,31). For all measurements, the stimulated echo pulse sequence was used in which the echo amplitude diffusional decay is given by (32)

$$A = A_0 \exp\left(-\gamma^2\delta^2 g^2 D\left(\Delta - \frac{\delta}{3}\right)\right), \quad (1)$$

where A_0 is the echo amplitude without applied gradients, γ is the gyromagnetic ratio, Δ is the time interval between gradient pulses, and δ and g are the duration and amplitude of the pulsed field gradients, respectively. In each diffusion experiment δ was varied, keeping all other parameters constant. The parameters were chosen so that the water signal was completely suppressed in order to observe only the signal from the lipids: $g = 1.15\ T/m$, δ varied from 1 to 12 ms, and Δ was 50–250 ms with the majority of the experiments made at 200 ms. The temperature was varied between 20 and 60°C and controlled within ±0.5°C by a heated air stream passing the sample. The CORE method for global analysis of the entire data set was used for the extraction of the lipid lateral diffusion coefficients (D_L values) (33). This method improves the quality of the evaluated data and provides the spectral features of each of the components in the multicomponent analyses. The CORE analysis gave one or two D_L values together with the corresponding spectral shapes. The distinction between whether there were one or two components was judged according to if there was a significant improvement in the normalized global error square sum with one or two components in the fit.

Differential scanning calorimetry

Measurements were performed on a MicroCal VP-DSC Microcalorimeter (Täby, Sweden). Samples of SM were hydrated to obtain a concentration of 2 mM and thoroughly mixed in a vortex stirrer. The samples were treated with at least five freeze-thaw cycles to obtain a homogeneous hydration of the lipid bilayers. DSC thermograms were obtained in heating and cooling scans from 1 to 60°C with a rate of 20°C/h. Four temperature scans were recorded, where the first scan was discarded to obtain a common thermal history of all samples. The appearance of the following scans was always identical.

RESULTS

In all the experiments the diffusional decay could be described by either one or two lipid diffusion components. The corresponding D_L values were unaffected for a change in the diffusion time between 50 and 250 ms. Fig. 2 shows an example of the diffusional decays obtained from the integrated intensities for DOPC/bSM/CHOL (37.5/37.5/25 mol %) at two temperatures. At 51°C the decay is monoexponential, while at 27°C it can only be satisfactorily described by the sum of two exponentials, yielding two D_L values.

Fig. 3, with D_L as a function of temperature, summarizes the results obtained for the three different SMs in mixtures with DOPC and CHOL. For the SM/water system the diffusional behavior is the same for all three SMs. D_L decreases

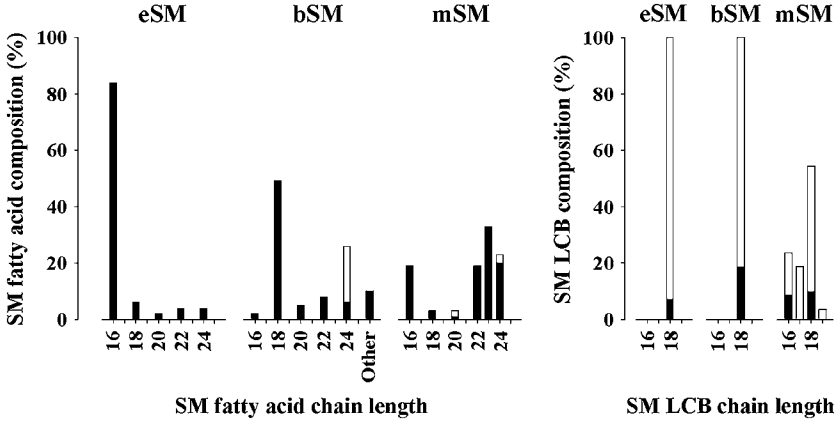

FIGURE 1 FA and LCB compositions for the three SMs. Solid bars correspond to saturated chains and open bars to unsaturated chains. For bSM, 10% of the fatty acids are unidentified and denoted by ''Other'' in the figure. Data for the LCB composition is taken from Ramstedt et al. (44) and that for the FA composition is obtained from the provider (*http://www.avantilipids.com/NaturalSphingomyelin.asp*). These values differ only slightly from those given in Ramstedt et al. (44).

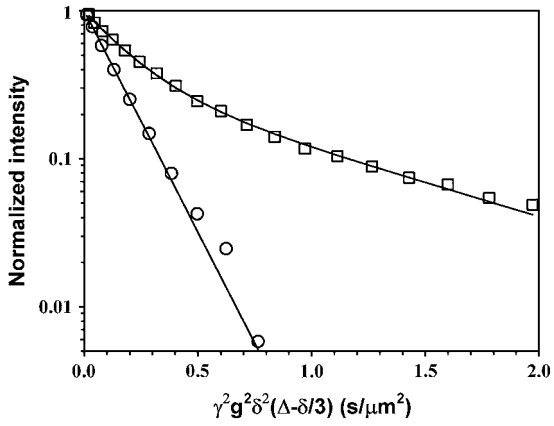

FIGURE 2 Plot of the integrated intensity of the spectra against $\gamma^2g^2\delta^2(\Delta-\delta/3)$ for a sample of DOPC/bSM/CHOL (37.5:37.5:25 mol %). The lines are best fits of the points to Eq. 1. (*Circles*) $T = 51°C$, $D = 10.5$ $\mu m^2/s$. (*Squares*) $T = 27°C$, $D_1 = 7.8$ $\mu m^2/s$ (67%), and $D_2 = 1.6$ $\mu m^2/s$ (33%). The results from analyzing the integrals generally gave the same results as the CORE analysis, but the latter was preferred due to the improved quality of the fits.

monotonically with decreasing temperature and the process is well described by an Arrhenius process (not shown) with an apparent activation energy of 40–44 kJ/mol (Fig. 3 *a*).

In the samples consisting of DOPC, SM, and CHOL the translational diffusion is characterized by one D_L at high temperatures and high CHOL concentrations. For CHOL concentrations roughly between 10 and 35 mol %, the decays for the eSM and bSM systems are biexponential at lower temperatures (Fig. 3, *b* and *c*). Thus, eSM and bSM are able to induce phase separation into l_d and l_o phases. However, the phase separation temperature is more than 10°C higher for the eSM system, indicating that the l_o phase has a higher thermodynamic stability with this lipid.

The apparent activation energies can only be estimated due to the scatter in the data and the small temperature intervals, but they seem to be higher in the l_o phase (50–90 kJ/mol) than in the l_d phase (20–40 kJ/mol) in accordance with earlier studies on raft systems (29,30).

At CHOL contents above 40 mol %, all three investigated systems behave roughly equally with only one diffusion coefficient and apparent activation energies in the range of 39–41 kJ/mol (Fig. 3 *d*).

No biexponential decays could be observed for mSM. This means that mSM is unable to induce phase separation (at least it will not partition into large domains; see also Discussion).

Fig. 4 tentatively summarizes the phase behavior for the eSM and bSM systems. The shaded area denotes the extension of the two-phase region obtained previously with eSM (29) and the thick line marks the corresponding region for bSM. The figure also shows measured points close to the phase border for the bSM system, where open circles denote a one-phase area and solid circles correspond to a two-phase region. Note that the lower boundary of the two-phase region in this figure denotes the temperature where the diffusion decay switches from biexponential to monoexponential. This does not exclude the possibility of two-phase coexistence below this line, since fast transverse relaxation in the ordered phase might reduce the fraction of the slow component below detection of the CORE analysis routine.

The results from the DSC measurements are also inserted into Fig. 4, where eSM has a transition at 38.8°C with a transition enthalpy (ΔH) of 6.3 kcal/mol, whereas the curve for bSM is considerably broader with the main peak at

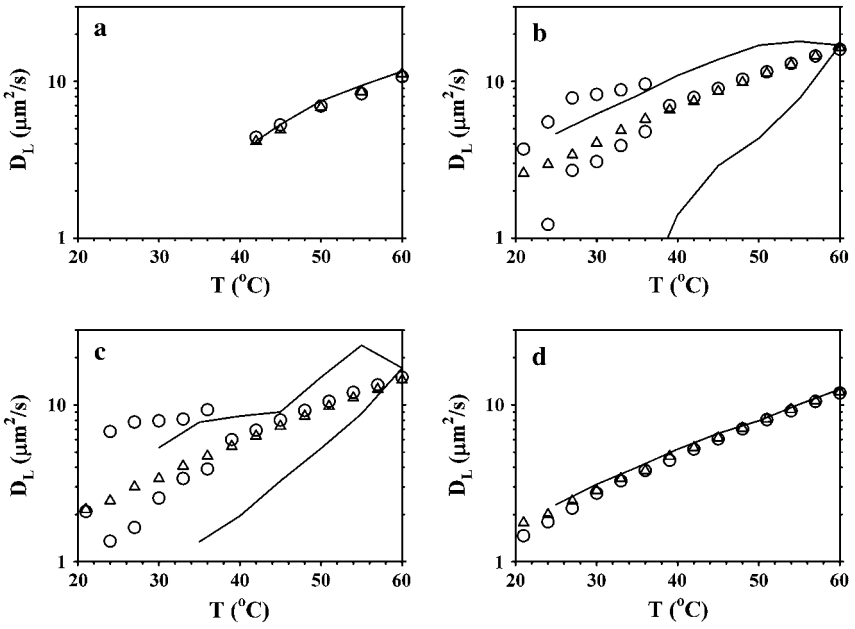

FIGURE 3 Obtained lateral diffusion coefficients versus temperature for some representative systems in one-phase and two-phase regions, containing eSM (*lines*, data taken from (29)), bSM (*circles*) and mSM (*triangles*). (*a*) SM, (*b*) DOPC/SM/CHOL (42.5/42.5/15 mol %), (*c*) DOPC/SM/CHOL (37.5/37.5/25 mol %), and (*d*) DOPC/SM/CHOL (30/30/40 mol %).

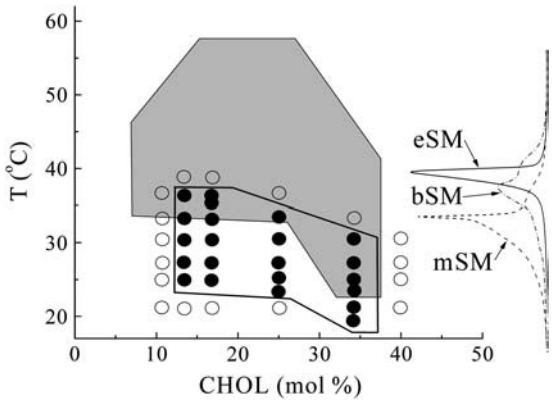

FIGURE 4 An overview tentatively showing the two-phase coexistence areas for the DOPC/eSM/CHOL system (*shaded area*), obtained from (29), and for the DOPC/bSM/CHOL system (*solid line*) from this study. Measured points for the DOPC/bSM/CHOL system are classified according to whether the diffusion decay was monoexponential (*open circles*) or biexponential (*solid circles*). The right inset shows the DSC curves for the three SMs.

36.8°C and a $\Delta H = 7.6$ kcal/mol. Finally, mSM features a curve composed of a sharp peak at 32.9°C with broad components on both sides of the main peak, and $\Delta H = 9.9$ kcal/mol. Both the transition temperatures and the enthalpies agree well with literature data (34,35).

DISCUSSION

Even though the obtained NMR signal contains overlapping contributions from the two phospholipids, the occurrence of two D_L values cannot simply be attributed to the motions of each of the two lipid species. Rather, previous investigations using isotopically labeled molecules have shown that all lipids (phospholipids as well as sterols) have the same D_L as long as they reside in the same phase (or domain) in the bilayer (9,36). Instead, two lipid D_L values indicate a lateral phase separation into the l_o and l_d phases in the bilayer. This conclusion is well supported from other studies in several raft-forming systems (9,29) and the observation of a diffusional decay with two components in pfg-NMR, therefore, provides a convenient method for investigation of the lateral phase separation process.

Since the obtained D_L values for eSM and bSM were insensitive to variations in the diffusion time between 50 and 250 ms, it is concluded that lipid exchange between l_o and l_d phases is slow on this timescale (29,37). This puts a lower limit to the domain sizes of slightly more than 1 μm, since the mean displacement of the lipids for the longest diffusion times is <3 μm. For the mSM system, on the other hand, only single D_L values were obtained. This could, at first sight, be ascribed to a microscopic phase separation with domain sizes much smaller than 1 μm, since then only a weighted mean value of the D_L values would be observed due to a fast exchange between the l_o and l_d phases (37). However, as a consequence of the different temperature dependence of D_L in the phases, this would give rise to curved lines in an Arrhenius plot because of a change in the relative amounts of the two phases, as the temperature is varied (30). Since this is not observed for mSM, we conclude that this system forms a homogeneous phase at all temperatures.

The tentative phase diagram in Fig. 4 shows the main differences in the raft-forming ability of the different SMs. The shaded area representing the two-phase coexistence of eSM extends to temperatures almost 20°C higher than for bSM, and it also reaches further down in CHOL concentration than for bSM, although the high limit of CHOL content seems to be the same. The high-temperature limit obtained for the two-phase region for the bSM system is in good agreement with observations by fluorescence microscopy (8), whereas that for the eSM is higher by almost 15°C in the pfg-NMR study. The results for the bSM system is also in qualitative agreement with fluorescence energy transfer measurements, although they find some support for domain formation at CHOL concentrations as high as 50 mol % (38). No two-phase coexistence could be observed for mSM, indicating that this molecule is even less raft-promoting than bSM. The difference in chemical structure for these molecules lies in the length and degree of unsaturation of the LCB and fatty acid (FA) chains. Fig. 1 shows the chain compositions of the three SMs. It is obvious that eSM has the most homogeneous composition, explaining the preferred use of this compound in model systems. The main difference between eSM and bSM is in the FAs, in which bSM has a larger proportion of long chains and also includes 20 mol % of the 24:1 unsaturated chain. mSM has a FA chain length distribution, which, on the average, is slightly longer than for bSM, but the main difference lies in the LCB, which for mSM contains large proportions of chains shorter than 18 carbons. The observed difference in ΔH is most probably a consequence of the difference in average chain lengths for the used SMs.

The broad DSC curves (see Fig. 4, *inset*) for bSM and mSM can be understood on the basis of the larger heterogeneity in the hydrocarbon chains of the molecules. The average increase in the chain length in bSM and mSM should result in an increase in the transition temperature of ~5°C (35), but this effect seems to be counteracted by the increased heterogeneity, the increased FA unsaturation in bSM, and by the decrease in the LCB length in mSM. Therefore, the main transition is lower for these compounds than for eSM.

The similar D_L values found for all the SM/^2H_2O systems (Fig. 3 *a*) indicate that there are only small differences in the SM-SM interactions. However, the fact that the various SMs in mixtures with DOPC and CHOL differ significantly in phase behavior indicates that other interactions are coming into play. Monolayer studies of CHOL oxidation (39) and desorption (27) rates have shown that CHOL associates more tightly to CHOL/SM mixed monolayers than to the corresponding CHOL/PC monolayer, and that there are differences

also within the lipid classes. Thus, unsaturated PCs protect CHOL from oxidation less well than saturated ones and bSM is less protective than eSM (39). Similar trends are also observed in a study of the surface compressional modulus of monolayers, a property that is correlated to the detergent resistance (40). In particular, it is found that bSM and DPPC have similar protective properties and this is consistent with our findings that the extension of the two-phase area in the DOPC/DPPC/CHOL system (8,9) has approximately the same high temperature limit as that for DOPC/bSM/CHOL, while that for the DOPC/eSM/CHOL system is significantly higher (Fig. 4 and (8,29)). However, a change in the FA chain lengths of the SMs seems to make very small differences in the desorption studies, and the introduction of a single double bond in the FA chain increases the desorption rate only for chain lengths <22 carbons (27). In this respect, it is difficult to see why the differences in chain length and saturation would make such a big difference in the raft-forming ability between eSM and bSM.

In an effort to elucidate the effect of the total degree of unsaturation in the system and also the importance of the ratio between the two phospholipids, a sample was prepared with a ratio of DOPC/bSM of 0.375:0.625 and a CHOL content of 25 mol %. This reduces the total unsaturation to values corresponding to that for DOPC/eSM with a molar ratio of 1:1. The results for DOPC/bSM = 0.375:0.625 were indistinguishable from those obtained for DOPC/bSM = 1:1, indicating that neither the ratio between DOPC and bSM, nor the degree of total unsaturation of the system, is critical for the upper and lower temperature boundaries of the two-phase area.

In searching for reasons for the formation of rafts it is possible that one important factor might be the larger homogeneity in the hydrocarbon chains for eSM, facilitating a tighter chain packing in the bilayer. It has been shown that the stereochemically pure *d*-erythro-SM packs more closely and reduces CHOL desorption more than the racemic mixture (28). Therefore, it seems reasonable to suggest that a homogeneous molecular SM structure promoting close packing conditions is of great importance for the raft-forming process. This might be the reason for the absence of any two-phase region in the mSM system, since mSM has an even more heterogeneous chain composition, which involves the LCB as well.

Recently, Epand and Epand (25) proposed a mechanism for the phase separation into l_o and l_d phases that did not specifically involve any SM-CHOL interactions. They showed that oleoyl-SM has a miscibility with CHOL that is only slightly greater than for the mostly saturated egg SM, indicating that the interaction between CHOL and SM does not depend on the degree of unsaturation (25). The fact that oleoyl-SM, in contrast to saturated SM, does not form domains with CHOL in the DOPC/oleoyl-SM/CHOL system was suggested to be caused by the greater miscibility of oleoyl-SM with DOPC. On the other hand, the miscibility of saturated SM with DOPC in the DOPC/SM/CHOL system is quite low, and therefore domains form. Moreover, recent studies indicate that CHOL seems not to be crucial for domain formation, since it can, at least partially, be displaced by another molecule, having a small headgroup and saturated chains, like a ceramide (41,42). This rather unexpected finding suggests that specific SM-CHOL interactions are not important for domain formation, but rather the ability of molecules to intercalate into a tightly packed network of, possibly, intermolecularly hydrogen-bonding SMs.

Miscibility of the compounds in the ordered and disordered phases can be used to rationalize the results obtained in this study if one relates the observed D_L values to the lipid packing in the membranes. A higher packing is expected to give rise to a diminished D_L because of the reduction in free area (43). This is indeed observed if one compares D_L values in the l_d and l_o phases. Fig. 5 shows D_L as a function of temperature for systems containing DOPC and/or SMs without CHOL, as well as with CHOL concentrations close to the borders of the one-phase areas (Fig. 4). The low D_L values found for pure SM membranes indicate that these are highly packed and the presence of hydrogen bonding might further reduce the lateral diffusion. Upon addition of DOPC, the diffusion coefficient goes up, almost to the level of pure DOPC bilayers. This means that the packing order (and hydrogen-bonding networks) is broken up by the introduction of DOPC into the SM bilayer. Gradual addition of CHOL is expected to restore the high order in the bilayer and this is manifested in a progressively decreasing D_L. At some point, the system breaks up into ordered and disordered phases due to the immiscibility of DOPC in an ordered phase. As seen in Fig. 5 *a*, all D_L values fall into one of two regions in the eSM systems; DOPC and DOPC/eSM have the high D_L values of a disordered phase, whereas eSM shows a much lower D_L because of the higher packing order in this membrane. For the one-phase regions of the two DOPC/eSM/CHOL mixtures, a higher CHOL content gives a lower D_L because of the ordering effect of CHOL. As the system enters the two-phase region, the observed diffusion coefficients are consistent with one disordered and one ordered phase.

The separation of the D_L values into two regions is not as distinct in the bSM system (Fig. 5 *b*) as for the eSM system. The trends for the one-phase systems are similar in both cases, but the D_L values in the two-phase area are scattered between the high- and low regions of diffusion coefficients. This further indicates that the larger heterogeneity of bSM disrupts the packing order in the bilayers, so that a clear distinction between order and disorder is difficult to make.

CONCLUSIONS

This study has shown that the differences in chain composition for the three SMs of natural origin give rise to large differences in the ability to form domains in mixtures with DOPC and CHOL. The fatty acid chain length distribution

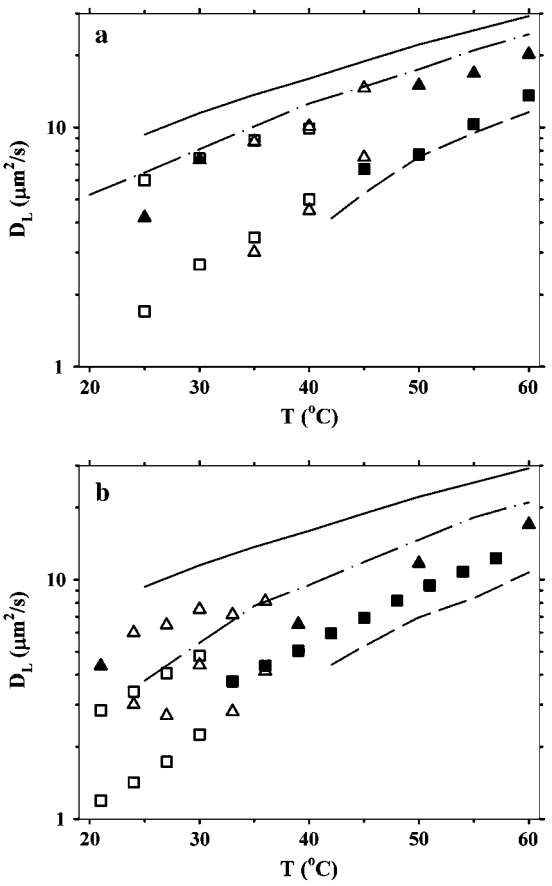

FIGURE 5 Diffusion coefficients as a function of temperature for some compositions for the (*a*) eSM (taken from (29,30)) and (*b*) bSM systems. The lines correspond to systems without CHOL, i.e., DOPC (*solid*), DOPC/SM (*dash-dot*), and SM (*dashed*). The symbols correspond to mixtures of DOPC/SM/CHOL, in which the CHOL contents are chosen to be in the outer edges of the two-phase areas: 8.7 (*triangles*) and 33 (*squares*) mol % for the eSM system, and 12.9 (*triangles*) and 33.5 (*squares*) mol % for the bSM system. Solid symbols are from the one-phase regions and open symbols from the two-phase regions.

and the presence of unsaturated chains in bSM lead to a smaller two-phase area than the more homogeneous eSM. mSM, which also has an inhomogeneous distribution of the LCB chain length, is unable to cause phase separation. Our findings suggest that the formation of l_o domains is to a large degree determined by the ability of the participating molecules to form a close-packed and highly ordered bilayer, and to a much lesser degree on the specific interactions between the molecules.

We gratefully acknowledge that this work was supported by The Magnus Bergvall Foundation, The Swedish Research Council, and The Knut and Alice Wallenberg Foundation.

REFERENCES

1. Rajendran, L., and K. Simons. 2005. Lipid rafts and membrane dynamics. *J. Cell Sci.* 118:1099–1102.
2. Simons, K., and D. Toomre. 2000. Lipid rafts and signal transduction. *Nat. Rev. Mol. Cell Biol.* 1:31–39.
3. Simons, K., and G. Van Meer. 1988. Lipid sorting in epithelial cells. *Biochemistry.* 27:6197–6202.
4. Ipsen, J. H., G. Karlström, O. G. Mouritsen, H. W. Wennerström, and M. J. Zuckermann. 1987. Phase equilibria in the phosphatidylcholine-cholesterol system. *Biochim. Biophys. Acta.* 905:162–172.
5. Vist, M. R., and J. H. Davis. 1990. Phase equilibria of cholesterol/dipalmitoylphosphatidylcholine mixtures: ^{2}H nuclear magnetic resonance and differential scanning calorimetry. *Biochemistry.* 29:451–464.
6. Brown, D. A., and J. K. Rose. 1992. Sorting of GPI-anchored proteins to glycolipid-enriched membrane subdomains during transport to the apical cell surface. *Cell.* 68:533–544.
7. Veatch, S. L., and S. L. Keller. 2002. Organization in lipid membranes containing cholesterol. *Phys. Rev. Lett.* 89:2681011–2681014.
8. Veatch, S. L., and S. L. Keller. 2003. Separation of liquid phases in giant vesicles of ternary mixtures of phospholipids and cholesterol. *Biophys. J.* 85:3074–3083.
9. Orädd, G., P. W. Westerman, and G. Lindblom. 2005. Lateral diffusion coefficients of separate lipid species in a ternary raft-forming bilayer: a pfg-NMR multinuclear study. *Biophys. J.* 89:315–320.
10. Brown, R. E. 1998. Sphingolipid organization in biomembranes: what physical studies of model membranes reveal. *J. Cell Sci.* 111:1–9.
11. Ramstedt, B., and J. P. Slotte. 2002. Membrane properties of sphingomyelins. *FEBS Lett.* 531:33–37.
12. Vaknin, D., M. S. Kelley, and B. M. Ocko. 2001. Sphingomyelin at the air-water interface. *J. Chem. Phys.* 115:7697–7704.
13. Veiga, M. P., J. L. R. Arrondo, F. M. Goni, A. Alonso, and D. Marsh. 2001. Interaction of cholesterol with sphingomyelin in mixed membranes containing phosphatidylcholine, studied by spin-label ESR and IR spectroscopies. A possible stabilization of gel-phase sphingolipid domains by cholesterol. *Biochemistry.* 40:2614–2622.
14. Ferguson-Yankey, S. R., D. Borchman, G. K. Taylor, D. B. DuPré, and M. C. Yappert. 2000. Conformational studies of sphingomyelins by NMR spectroscopy. I. Dihydrosphingomyelin. *Biochim. Biophys. Acta.* 1467:307–325.
15. Maulik, P. R., and G. G. Shipley. 1996. N-palmitoyl sphingomyelin bilayers: structure and interactions with cholesterol and dipalmitoylphosphatidylcholine. *Biochemistry.* 35:8025–8034.
16. Maulik, P. R., P. K. Sripada, and G. G. Shipley. 1991. Structure and thermotropic properties of hydrated N-stearoyl sphingomyelin bilayer membranes. *Biochim. Biophys. Acta.* 1062:211–219.
17. Petrach, H. I., S. W. Dodd, and M. F. Brown. 2000. Area per lipid and acyl length distributions in fluid phosphatidylcholines determined by ^{2}H NMR spectroscopy. *Biophys. J.* 79:3172–3192.
18. Shipley, G. G., L. S. Avecilla, and D. M. Small. 1974. Phase behavior and structure of aqueous dispersions of sphingomyelin. *J. Lipid Res.* 15:124–131.
19. Chiu, S. W., S. Vasudevan, E. Jakobsson, R. J. Mashi, and H. L. Scott. 2003. Structure of sphingomyelin bilayers: a simulation study. *Biophys. J.* 85:3624–3635.
20. Hyvönen, M. T., and P. T. Kovanen. 2003. Molecular dynamics simulation of sphingomyelin bilayer. *J. Phys. Chem.* 107:9102–9108.
21. Mombelli, E., R. Morris, W. Taylor, and F. Fraternali. 2003. Hydrogen bonding propensities of sphingomyelin in solution and in a bilayer assembly: a molecular dynamics simulation. *Biophys. J.* 84:1507–1517.
22. Kelashvili, G. A., and H. L. Scott. 2004. Combined Monte Carlo and molecular dynamics simulation of hydrated 18:0 sphingomyelin-cholesterol bilayers. *J. Chem. Phys.* 120:9841–9847.
23. Térová, B., R. Heczko, and J. P. Slotte. 2005. On the importance of the phosphocholine methyl groups for sphingomyelin/cholesterol interactions in membranes: a study with ceramide phosphoethanolamine. *Biophys. J.* 88:2661–2669.

24. Bittman, R., C. R. Kasireddy, P. Mattjus, and J. P. Slotte. 1994. Interaction of cholesterol with sphingomyelin in monolayers and vesicles. *Biochemistry*. 33:11776–11781.

25. Epand, R. M., and R. F. Epand. 2004. Non-raft forming sphingomyelin-cholesterol mixtures. *Chem. Phys. Lipids*. 132:37–46.

26. Mattjus, P., and J. P. Slotte. 1996. Does cholesterol discriminate between sphingomyelin and phosphatidylcholine in mixed monolayers containing both phospholipids? *Chem. Phys. Lipids*. 81:69–80.

27. Ramstedt, B., and J. P. Slotte. 1999. Interaction of cholesterol with sphingomyelins and acyl-chain-matched phosphatidylcholines: a comparative study of the effect of the chain length. *Biophys. J*. 76:908–915.

28. Ramstedt, B., and J. P. Slotte. 1999. Comparison of the biophysical properties of racemic and *d-erythro-N-acyl* sphingomyelins. *Biophys. J*. 77:1498–1506.

29. Filippov, A., G. Orädd, and G. Lindblom. 2004. Lipid lateral diffusion in ordered and disordered phases in raft mixtures. *Biophys. J*. 86:891–896.

30. Filippov, A., G. Orädd, and G. Lindblom. 2003. The effect of cholesterol on the lateral diffusion of phospholipids in oriented bilayers. *Biophys. J*. 84:3079–3086.

31. Orädd, G., and G. Lindblom. 2004. Lateral diffusion studied by pulsed field gradient NMR on oriented lipid membranes. *Magn. Reson. Chem*. 42:123–131.

32. Tanner, J. E. 1970. Use of the stimulated echo in NMR diffusion studies. *J. Chem. Phys*. 52:2523–2526.

33. Stilbs, P., K. Paulsen, and P. C. Griffiths. 1996. Global least-squares analysis of large, correlated spectral data sets: application to component-resolved FT-PGSE NMR spectroscopy. *J. Phys. Chem*. 100:8180–8189.

34. Malmsten, M., M. Bergenståhl, B. Nyberg, and G. Odham. 1994. Sphingomyelin from milk—characterization of liquid-crystalline, liposome and emulsion properties. *J. Am. Oil Chem. Soc*. 71:1021–1026.

35. Koynova, R., and M. Caffrey. 1995. Phases and phase transitions of the sphingolipids. *Biochim. Biophys. Acta*. 1255:213–236.

36. Orädd, G., G. Lindblom, and P. W. Westerman. 2002. Lateral diffusion of cholesterol and dimyristoylphosphatidylcholine in a lipid bilayer measured by pulsed field gradient NMR spectroscopy. *Biophys. J*. 83:2702–2704.

37. Kärger, J., H. Pfeifer, and W. Heink. 1988. Principles and application of self-diffusion measurements by nuclear magnetic resonance. *In* Advances in Magnetic and Optical Resonance. W.S. Warren, editor. Academic Press, San Diego, CA. 1–89.

38. Silvius, J. R. 2003. Fluorescence energy transfer reveals microdomain formation at physiological temperatures in lipid mixtures modeling the outer leaflet of the plasma membrane. *Biophys. J*. 85:1034–1045.

39. Slotte, J. P. 1992. Enzyme-catalyzed oxidation of cholesterol in mixed phospholipid monolayers reveals the stoichiometry at which free cholesterol clusters disappear. *Biochemistry*. 31:5472–5477.

40. Li, X.-M., M. M. Momsen, J. M. Smaby, H. L. Brockman, and R. E. Brown. 2001. Cholesterol decreases the interfacial elasticity and detergent solubility of sphingomyelin. *Biochemistry*. 40:5954–5963.

41. Björkqvist, Y. J. E., T. K. M. Nyholm, J. P. Slotte, and B. Ramstedt. 2005. Domain formation and stability in complex lipid bilayers as reported by cholestatrienol. *Biophys. J*. 88:4054–4063.

42. Megha and E. London. 2004. Ceramide selectively displaces cholesterol from ordered lipid domains (rafts). Implications for lipid raft structure and function. *J. Biol. Chem*. 279:9997–10004.

43. Almeida, P. F. F., W. L. C. Vaz, and T. E. Thompson. 1992. Lateral diffusion in the liquid phases of dimyristoylphosphatidylcholine/cholesterol bilayers: a free volume analysis. *Biochemistry*. 31:6739–6747.

44. Ramstedt, B., P. Leppimaki, M. Axberg, and J. P. Slotte. 1999. Analysis of natural and synthetic sphingomyelins using high-performance thin-layer chromatography. *Eur. J. Biochem*. 266:997–1002.